

Low-energy (<20 eV) and high-energy (1000 eV) electron-induced methanol radiolysis of astrochemical interest

Kristal K. Sullivan, Mavis D. Boamah, Katie E. Shulenberger, Sitara Chapman, Karen E. Atkinson, Michael C. Boyer and Christopher R. Arumainayagam †

Accepted 2016 March 10. Received 2016 March 8; in original form 2014 September 29

ABSTRACT

We report the firs infrared study of the low-energy (<20 eV) electron-induced reactions of condensed methanol. Our goal is to simulate processes which occur when high-energy cosmic rays interact with interstellar and cometary ices, where methanol, a precursor of several prebiotic species, is relatively abundant. The interactions of high-energy radiation, such as cosmic rays ($E_{\rm max} \sim 10^{20}$ eV), with matter produce large numbers of low-energy secondary electrons, which are known to initiate radiolysis reactions in the condensed phase. Using temperature programmed desorption (TPD) and infrared reflectio absorption spectroscopy (IRAS), we have investigated low-energy (5–20 eV) and high-energy (~1000 eV) electron-induced reactions in condensed methanol (CH₃OH). IRAS has the benefit that it does not require thermal processing prior to product detection. Using IRAS, we have found evidence for the formation of ethylene glycol (HOCH₂CH₂OH), formaldehyde (CH₂O), dimethyl ether (CH₃OCH₃), methane (CH₄), carbon dioxide (CO₂), carbon monoxide (CO), and the hydroxyl methyl radical (•CH₂OH) upon both low-energy and high-energy electron irradiation of condensed methanol at \sim 85 K. Additionally, TPD results, presented herein, are similar for methanol film irradiated with both 1000 eV and 20 eV electrons. These IRAS and TPD finding are qualitatively consistent with the hypothesis that high-energy condensed phase radiolysis is mediated by low-energy electron-induced reactions. Moreover, methoxymethanol (CH₃OCH₂OH) could serve as a tracer molecule for electron-induced reactions in the interstellar medium. The results of experiments such as ours may provide a fundamental understanding of how complex organic molecules are synthesized in cosmic ices.

Key words: astrochemistry-molecular processes-radiation mechanisms: non-thermal-ISM: clouds-cosmic rays.

1 INTRODUCTION

Methanol (CH₃OH) is of astrochemical interest because of its relatively high abundance in protostar environments (Maret et al. 2005), interstellar clouds (Friberg et al. 1988), and comets (Bockeleemorvan et al. 1991). Relative to that of water ice, observed interstellar methanol ice abundance values range from 1 per cent to as high as 30 per cent (Grim et al. 1991; Gibb et al. 2004; Oberg et al. 2011). Moreover, methanol is thought to be an important precursor not only to simple species such as methyl formate (HCOOCH₃) and

dimethyl ether (CH₃OCH₃), but also to many prebiotic species such as simple sugars and amino acids (Allamandola & Hudgins 2000; Hollis, Lovas and Jewell 2000; Andrade et al. 2009). It has been proposed that CH₃OH formation occurs through the successive hydrogenation of CO molecules in ice mantles encasing interstellar dust grains (Watanabe, Shiraki & Kouchi 2003). Laboratory experiments simulating these processes have demonstrated the formation of formaldehyde (CH₂O) and methanol in amounts consistent with observed abundances in the interstellar medium (ISM) (Watanabe et al. 2003).

Remnants of older generations of stars, interstellar clouds of gas, dust, and ice become the building blocks of protostellar discs, from which new stars, planets, asteroids, comets, and other macroscopic objects form (Ehrenfreund & Charnley 2000; Mannings, Boss & Russell 2000; Herbst 2014). Observations at infrared,

¹Department of Chemistry, Wellesley College, Wellesley, MA 02481, USA

²Science and Engineering Department, Bunker Hill Community College, Boston, MA 02129, USA

^{*} Present Address: Department of Physics, Clark University, Worcester, MA 01610

[†] E-mail: mboyer@clarku.edu (MCB); carumain@wellesley.edu (CRA)

submillimetre, millimetre, and radio frequencies show that a large variety of organic molecules are present in these interstellar clouds (Mannings et al. 2000; Garrod, Widicus & Herbst 2008). In fact, star-forming regions within dark, dense molecular clouds are define by a relative abundance of organic molecules such as methanol (Garrod et al. 2008). Organic molecular classes identifie within these protostellar hot cores and hot corinos include nitriles, aldehydes, alcohols, acids, ethers, ketones, amines, and amides (Irvine, Goldsmith & Hjalmarson 1987; Olano, Wlamsley & Wilson 1988; van Dishoeck, Jansen & Phillips 1993). Although the majority of identifie species consist of only a few atoms, larger molecules such as fullerenes and polycyclic aromatic hydrocarbons have also been observed in several different regions of the ISM (Allamandola & Hudgins 2000; Mannings et al. 2000; García-Hernández, Cataldo & Manchado 2013).

Multiple reaction pathways for the formation of molecules in the ISM environment must be available given the extreme variations in interstellar physical conditions, such as densities ranging from 10² to 10⁸ hydrogen atoms cm⁻³ and temperatures ranging from 10 to 10 000 K (Mangum & Wootten 1993; Ehrenfreund & Charnley 2000). Gas-phase reactions, surface reactions on bare dust grains, and UV-induced chemistry in ice mantles are thought to be the three main mechanisms for chemical synthesis in the ISM (Charnley, Tielens & Millar 1992; Herbst 2014).

Barrier-less gas-phase reactions in the ISM are sufficientl effi cient to account for the formation of simple species such as CO, N2, O2, C2H4, HCN, and simple carbon chains (Herbst 1995). However, studies have shown that gas-phase processes are much too inefficien to account for the observed abundance of species such as methyl formate (HCOOCH₃) in star-forming regions, suggesting that gas-phase processes play only a minor role in the formation of more complex species (Horn et al. 2004). Although surface reactions on carbonaceous or silicaceous dust grains in diffuse interstellar clouds are responsible for the synthesis of molecular hydrogen (Vidali 2013), experiments of surface hydrogenation reactions have shown the favoured mechanism to be the dissociation, rather than the synthesis, of complex molecules (Bisschop et al. 2007). Thus, surface reactions on bare dust grains may serve to slow the buildup of complex molecules. In contrast, in ice mantles surrounding dust grains found in cold, dark, dense molecular clouds, synthesis of complex organic molecules (COM) is thought to occur via both surface and bulk reactions.

According to a recent publication, 'models show that photochemistry in ices followed by desorption may explain the observed abundances' of gas-phase complex molecules detected in hot cores (Oberg et al. 2009). The interstellar UV radiation f eld, however, is not able to penetrate into the dark interior of dense molecular clouds (Prasad & Tarafdar 1983). Following excitation by secondary electrons produced by cosmic rays, H₂ molecules decay to the ground electronic state by emitting UV photons, leading to a cosmic rayinduced UV radiation f eld within the dark, dense molecular clouds (Prasad & Tarafdar 1983). These cosmic ray-induced UV photons are thought to photo-process ice mantles surrounding dust grains within the protostar environment (Prasad & Tarafdar 1983).

In addition to UV light, high-energy radiation (e.g., cosmic rays and γ -rays) is also incident on interstellar ices. The interaction of high-energy radiation with condensed matter results in the formation of copious numbers (\sim 4 × 10⁴ electrons per MeV of energy deposited) of low-energy secondary electrons, which form distinct energetic species that are thought to promote a variety of radiation-induced chemical reactions (Kaplan & Miterev 1987). The majority of these secondary electrons have energies below 15 eV,

and dissociate neutral molecules via one of three mechanisms: (1) dissociative electron attachment (DEA), (2) electron impact excitation, or (3) electron impact ionization (Arumainayagam et al. 2010). The three electron-induced molecular dissociative mechanisms are illustrated below for a generic neutral molecule AB.

$$e^- + AB \rightarrow AB^{-*} \rightarrow \cdot A + B^-$$
 (1)

$$e^- + AB \rightarrow AB^* + e^- \rightarrow \cdot A^* + \cdot B + e^-$$
 (2)

$$e^{-} + AB \rightarrow AB^{+*} + 2e^{-} \rightarrow A + B^{+*} + 2e^{-}$$
. (3)

DEA (equation 1), a resonant process occurring at low electron energies (0 to 15 eV), is characterized by the initial capture of an electron by a molecule to form a transient negative ion, which subsequently dissociates into a radical and an anion (Arumainayagam et al. 2010). Unlike electrons, photons cannot be captured into resonant negative ion states. In contrast, both photons and electrons can induce excitation and ionization. Electron impact electronic excitation followed by dipolar dissociation (equation 2) and electron impact ionization followed by fragmentation (equation 3) occur at electron energies typically above 3 and 10 eV, respectively.

The secondary electrons resulting from the interaction of highenergy radiation (e.g., cosmic rays) with matter are characterized by the majority of electrons having energies below ~ 15 eV (Fig. 1a). For a generic molecule, the dissociation cross-section as a function of incident electron energy (Fig. 1b) shows resonances due to DEA at low (<15 eV) electron energies, followed by a monotonic increase at higher electron energies due to available electron impact excitation and ionization dissociation pathways. Multiplying the secondary electron energy distribution by the dissociation crosssection gives the dissociation yield as a function of electron energy (Fig. 1c). Even though the dissociation probability increases above a threshold of ~ 10 eV for a typical molecule, the yield function indicates that dissociation due to secondary electrons is far more likely at energies below \sim 15 eV (Arumainayagam et al. 2010). According to a recent publication, 'it is appropriate to suggest that low-energy electrons are the most important species in radiation chemistry' (Pimblott & LaVerne 2007).

Processing of interstellar, cometary, and planetary ices likely involves high-energy radiation-induced low-energy electrons. While

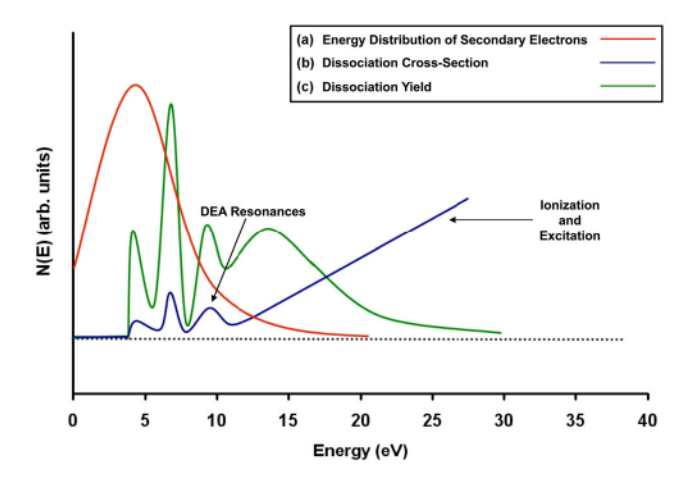


Figure 1. Schematic of (a) energy distribution of secondary electrons generated during a primary ionizing event; (b) cross-section for electron-induced dissociation for a typical molecule; (c) dissociation yield as a function of electron energy for a typical molecule (Arumainayagam et al. 2010).

the mean free paths of low-energy (18–68 eV) electrons in condensed water and methanol are $\sim\!13$ and $\sim\!10$ Å, respectively (Kurtz et al. 1986), the penetration depth of light ions can be as high as $10^6~\mu m$ in interstellar ices, which are typically less than 1 μm thick (de Barros et al. 2014). Therefore, we propose that cosmic-ray-induced low-energy electron processing of interstellar ices may occur via three mechanisms (Cuppen 2014): (1) the interaction of cosmic rays with gaseous molecular hydrogen produces low-energy electrons that can interact with the surface (top few molecular layers) of cosmic ices, (2) the interaction of cosmic rays with molecules within ices generates a cascade of low-energy electrons which can interact with the surface and the bulk of the ice mantles, (3) the interaction of the cosmic rays with the dust grain beneath the ice mantle engenders low-energy electrons that can interact with the bottom ice layers in contact with the dust grain.

Based on post-irradiation temperature programmed desorption (TPD) experiments, we have recently shown that low-energy (<20 eV) electron processing of methanol ices essentially produces the same products as UV photolysis of condensed methanol (Boamah et al. 2014). In the work presented herein, we have extended our previously published work to include the use of postirradiation IR for product identification While both techniques allow us to identify the radiolysis products of methanol, in contrast to TPD, infrared reflectio absorption spectroscopy (IRAS) has an advantage in that it does not require thermal processing prior to product detection. In addition, we have extended our studies of low-energy (<20 eV) electrons to high-energy (1000 eV) electrons. In the post-irradiation TPD and infrared spectroscopy results presented herein, we demonstrate that the same radiolysis products result from irradiation of condensed methanol with low-energy (<20 eV) and high-energy (~1000 eV) electrons. These qualitative finding indicate that high-energy radiation-induced changes may be attributable to low-energy secondary electron interactions with condensed matter. Hence, our results suggest that cosmic-rayinduced low-energy electrons very likely play an important role in the synthesis of complex molecules in the ISM.

2 EXPERIMENTAL SECTION

Experiments were performed in a custom-designed stainless steel ultrahigh vacuum (UHV) chamber with a base pressure of 5×10^{-10} Torr, previously described in detail (Harris et al. 1995). A Mo(110) single crystal substrate was mounted on a precision sample manipulator capable of x-, y-, and z-translations. Polar rotation of the crystal mount was provided by a differentially pumped rotary feedthrough. The crystal substrate could be cooled to $\sim\!85$ K with liquid nitrogen and heated to 800 K radiatively or to 2200 K by electron bombardment. Temperature measurements were made using a tungsten—rhenium, W-5 per cent Re versus W-26 per cent Re thermocouple spot welded to the edge of the crystal. The crystal was routinely cleaned by heating to 2200 K, exceeding the desorption temperature of oxygen.

All samples [CH₃OH (Aldrich, 99.9+ per cent), ¹³CH₃OH (Aldrich, 99 per cent), CH₃CH₂OH (Pharmco, anhydrous absolute), HCOOCH₃ (Aldrich, anhydrous 99 per cent), CH₃OCH₃ (Aldrich, 99 per cent), HOCH₂CH₂OH, (Aldrich, anhydrous 99.8 per cent) HCOCH₂OH (Aldrich, crystalline dimer), and CH₃COOH (EMD, glacial)] were stored in cleaned (baked) Schlenk tubes and degassed by three freeze-pump-thaw cycles before use. The two exceptions were (1) HCOCH₂OH, a solid dimer sample which was gently heated to produce monomer fragments before introduction to the

chamber, and (2) CH₃OCH₃, which was packaged in a pressurized canister and introduced directly into the UHV chamber.

Dosers with precision leak valves allowed for controlled deposition of methanol onto the Mo(110) crystal surface. TPD experiments in the absence of electron irradiation were used to determine the coverage of $\mathrm{CH_3OH}$. One monolayer (1 ML) is define as the coverage achieved by the maximum exposure of the adsorbate that does not yield a multilayer peak. Film thickness (20–100 ML) was sufficient to rule out any contribution from Mo surface interactions. To minimize charging of film during irradiation with low-energy electrons, we used 20 ML film for post-irradiation TPD experiments. For better signal-to-noise ratio, we used 100 ML film for post-irradiation IRAS experiments. Multilayers of methanol at 85 K form an amorphous solid (glass), because crystallization of methanol occurs only above 128 K (Dempster & Zerbi 1971).

An FRA-2 \times 1–2 electron gun (Kimball Physics Inc.) was used to irradiate condensed methanol film on the crystal substrate. The transmitted current was set at 2.0 μ A (electron dose of 2.4 \times 10³ μ C) on the clean crystal for most experiments. Incident electron energy was varied between 5 and 1000 eV. Our choice of 5 eV for the minimum incident electron energy was dictated by the fact that at electron energies below \sim 10 eV, electron impact ionization is not a viable mechanism for product formation.

Post-irradiation IRAS measurements were performed using a recently installed TENSOR 27 Fourier Transform Infrared (FTIR) spectrometer (Bruker Optics) equipped with a liquid nitrogen-cooled mercury cadmium telluride detector. A background spectrum (1000 scans at 8 cm⁻¹ resolution) of the clean crystal was subtracted from all sample IRAS spectra. Unless otherwise noted, all sample spectra were collected at 8 cm⁻¹ resolution with coaddition of 250 scans for each spectrum.

After irradiation of methanol film with electrons, TPD measurements were also performed using a Hidden IDP Series 500 quadrupole mass spectrometer. Five or fewer mass-to-charge ratios were monitored during typical TPD experiments in order to optimize the signal-to-noise ratio while allowing for identificatio of radiolysis products. TPD experiments conducted in the absence of electron irradiation served as control experiments.

3 RESULTS AND DISCUSSION

Multiple methods based on IRAS were utilized to identify low- and high-energy electron-induced nascent radiolysis products formed at 85 K within methanol thin films First, IR peak positions were compared to previously published values for the radiolysis/photolysis products of condensed methanol. Secondly, these peak assignments were further verifie by annealing experiments during which the irradiated CH3OH thin fil was heated to various temperatures before IR analysis at 85 K. The temperatures corresponding to the loss of IR peaks were compared with previously recorded radiolysis product desorption temperatures (Harris et al. 1995; Boamah et al. 2014). Thirdly, mixtures of CH₃OH with approximately 10–30 per cent of the potential radiolysis product were dosed onto the crystal at 85 K. IR spectra of these unirradiated, mixed thin film were used as additional evidence for peak assignments in electron-irradiated condensed methanol. Fourthly, IR spectra of irradiated ¹³CH₃OH were used to further verify radiolysis product identification for species such as CO and CO2, which are significan contaminants in UHV chambers.

As described in detail elsewhere (Boamah et al. 2014), the identification of electron-induced methanol radiolysis species via post-irradiation TPD were based on (1) comparison to known mass

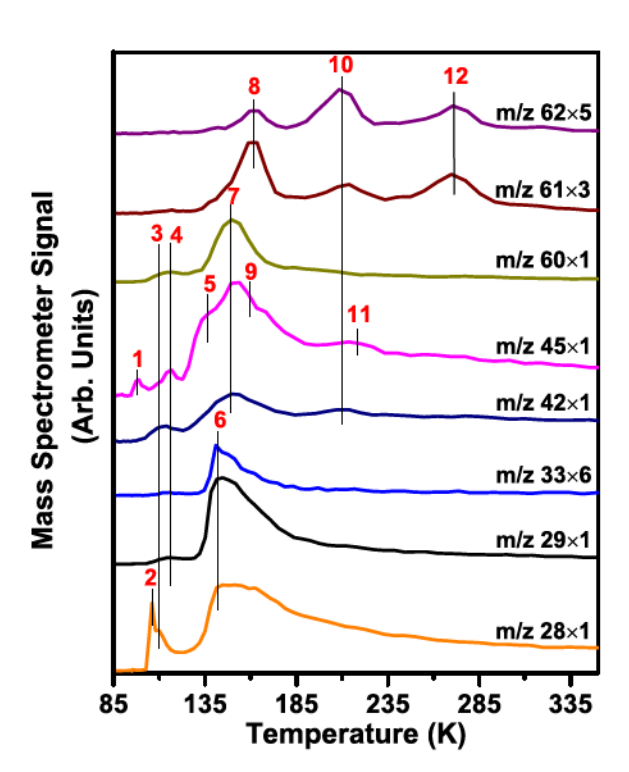


Figure 2. Post irradiation TPD data for 20 monolayers of 12 CH₃OH irradiated with 1000 eV electrons for 5 s at a transmitted current of 2 μ A (f ux $\approx 2 \times 10^{13}$ electrons cm⁻² s⁻¹ and f uence $\approx 1 \times 10^{14}$ electrons cm⁻²) show several desorption features: (1) dimethyl ether (CH₃OCH₃), (2) carbon monoxide (CO), (3) methyl formate (HCOOCH₃), (4) glycolaldehyde (HOCH₂CHO), (5) unknown, (6) methanol, (7) acetic acid (CH₃COOH), (8) methoxymethanol (CH₃OCH₂OH), (9) ethanol (CH₃CH₂OH), (10) ethylene glycol ((CH₂OH)₂), (11) glycolic acid (HOCH₂CO₂H), (12) 1,2,3-propanetriol (HOCH₂CHOHCH₂OH, glycerol). We note that methanol has a natural abundance of 13 C (about 1%) which allows us to monitor m/z = 33 to detect methanol in our experiments. Plots vertically offset for clarity.

spectra, (2) TPD data for methanol film containing the suspected radiolysis product, (3) results of analogous experiments with methanol isotopologues (13CH3OH and CD3OD), and (4) trends in boiling points and desorption temperatures. Despite the use of these methods, several of our identification of electron-induced methanol radiolysis products are not unambiguous because of (1) the multitude of methanol radiolysis products, (2) small reaction yields which were dependent on fil thickness, irradiation time, and incident electron energy, (3) closeness in desorption temperatures of some radiolysis products, and (4) the inability to monitor mass spectral fragments (e.g., m/z = 31) that were common to both methanol and some radiolysis products. Results of TPD experiments conducted following high-energy (1000 eV) and low-energy (20 eV) electron irradiation of methanol thin film are shown in Figs 2 and 3, respectively. To improve clarity, not all mass spectral fragments monitored are shown in these two f gures. As a result, positions of some vertical lines used to identify peaks are not obvious in Fig. 3.

3.1 Ethylene glycol (HOCH2CH2OH) formation

Based on the results of post-irradiation TPD, ethylene glycol was identifie as a radiolysis product following irradiation of condensed methanol with high-energy (1000 eV) electrons (Fig. 2). We have previously demonstrated that irradiation of methanol ices by elec-

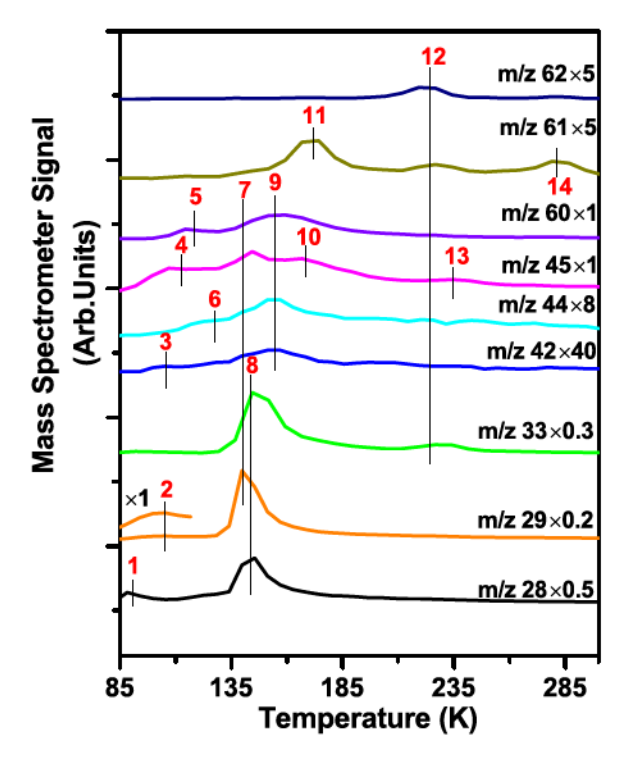


Figure 3. Post-irradiation TPD data for 20 monolayers of $^{12}\text{CH}_3\text{OH}$ irradiated with 20 eV electrons for 20 min at a transmitted current of 2 μA (flu $\approx 2 \times 10^{13}$ electrons cm $^{-2}$ s $^{-1}$ and fuence $\approx 3 \times 10^{16}$ electrons cm $^{-2}$) show several desorption features: (1) CO (background), (2) formaldehyde (H₂CO), (3) unknown, (4) dimethyl ether (CH₃OCH₃), (5) methyl formate (HCOOCH₃), (6) acetaldehyde (CH₃CHO), (7) glycolaldehyde (HOCH₂CHO), (8) methanol (CH₃OH), (9) acetic acid (CH₃COOH), (10) ethanol (CH₃CH₂OH), (11) methoxymethanol (CH₃OCH₂OH), (12) ethylene glycol ((CH₂OH)₂), (13) glycolic acid (HOCH₂CO₂H), and (14) 1, 2, 3-propanetriol (HOCH₂CHOHCH₂OH). We note that methanol has a natural abundance of 13 C (about 1%) which allows us to monitor mtz = 33 to detect methanol in our experiments. Plots vertically offset for clarity (Boamah et al. 2014).

trons with energies as low as 5 eV results in the formation of ethylene glycol (Boamah et al. 2014).

Even in the absence of the thermal processing characteristic of TPD, post-irradiation IR spectra demonstrate the formation of ethylene glycol (HOCH2CH2OH) at 85 K upon low-energy (20 eV) and high-energy (900 eV) electron irradiation of condensed methanol (Fig. 4). Ethylene glycol formation at 85 K was verifie by the presence of a prominent IR peak at \sim 1092 cm⁻¹, as well as weaker peaks at ~890 and ~865 cm⁻¹, observed following electron irradiation of condensed methanol. Ethylene glycol production was observed via IR spectroscopy when methanol film were irradiated with electrons with energies as low as 7 eV (electron dose of $2.4 \times 10^3 \mu C$), suggesting that electron impact ionization cannot be the sole mechanism for ethylene glycol formation. During annealing experiments, IR peaks associated with ethylene glycol disappeared between 200 and 250 K, consistent with the ~210 K ethylene glycol desorption temperature found during TPD following low-energy electron irradiation of condensed methanol. Furthermore, IR spectra of thin film formed from a mixture of ~ 10 per cent (v/v) ethylene glycol in CH₃OH dosed onto the Mo(110) crystal at 85 K evinced prominent peaks that were consistent with features attributed to ethylene glycol in the irradiated CH3OH thin film Our IR identificatio of ethylene glycol formation following low- and high-energy electron irradiation of condensed methanol is consistent with previous IR

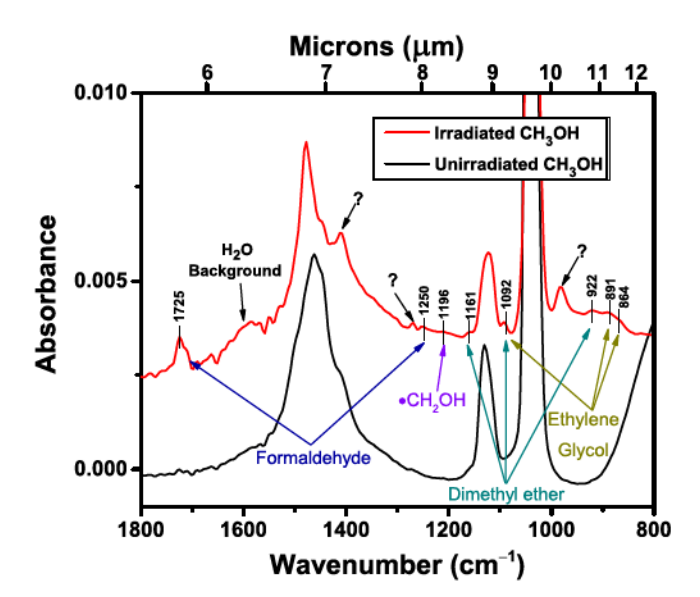


Figure 4. IRAS spectra of 100 ML of unirradiated (black curve) and irradiated (14 eV electrons for 20 min at a transmitted current of 2 μ A) (red curve) condensed CH₃OH.

studies involving high-energy electrons (Bennett et al. 2007), UV (Gerakines, Schutte & Ehrenfreund 1996; Oberg et al. 2009), X-ray (Chen et al. 2013), and proton (Hudson & Moore 2000) irradiation of methanol ices.

Methanol radiolysis leading to ethylene glycol formation has been previously attributed to the dimerization of two hydroxymethyl (•CH₂OH) radicals (Getoff et al. 1993). The absence of ethylene glycol in high-energy electron-irradiated methanol ice at 30 K (Jheeta et al. 2013) is consistent with heavy radicals such as hydroxymethyl radicals requiring higher temperatures for facile diffusion. Given that copious numbers of low-energy electrons are produced by the interactions of high-energy radiation, electron impact electronic excitation is likely the dominant mechanism for the formation of hydroxymethyl radicals during the high-energy radiolysis of methanol, as we have described in detail elsewhere (Boyer et al. 2014).

3.2 Formaldehyde (H2CO) formation

Formaldehyde (H₂CO) formation at 85 K following electron irradiation of condensed methanol was confirme by IR peaks at 1725 and 1250 cm⁻¹ (Fig. 4). Formation of formaldehyde was seen after irradiation with electrons with energies as low as 9 eV (electron dose of $2.4 \times 10^3 \,\mu\text{C}$). Results of annealing experiments showed the disappearance of formaldehyde IR peaks between 120 and 135 K, slightly above the desorption temperature of ~115 K reported in our previous post-irradiation TPD study of condensed methanol (Boamah et al. 2014). The prominent IR peak at ~1725 cm⁻¹ has been observed following radiolysis/photolysis of condensed methanol (Allamandola, Sandford & Valero 1988; Gerakines et al. 1996; Palumbo, Castorina & Strazzulla 1999; Hudson & Moore 2000; Baratta, Leto & Palumbo 2002; Oberg et al. 2009; de Barros et al. 2011; Chen et al. 2013; Jheeta et al. 2013).

Formaldehyde is thought to be produced through the combination of \cdot H and \cdot HCO radicals and/or disproportionation of the hydroxymethyl radicals within the irradiated CH₃OH thin fil (Getoff et al. 1993). Facile \cdot H radical diffusion possible at \sim 10 K (Watanabe et al. 2003) probably accounts for the detection of

formaldehyde at temperatures as low as 11 K following irradiation of condensed methanol with high-energy (5000 eV) electrons (Bennett et al. 2007).

3.3 Dimethyl ether (CH₃OCH₃) formation

Results of TPD experiments conducted following high-energy (1000 eV) electron irradiation of condensed CH₃OH demonstrated desorption features which we attribute to dimethyl ether (Fig. 2). We have previously demonstrated that irradiation of methanol ices by electrons with electron energies as low as 7 eV results in the formation of dimethyl ether (Boamah et al. 2014).

The electron-induced production of dimethyl ether (CH₃OCH₃) at 85 K from condensed methanol was confirme by the prominent IR peak at $1092~{\rm cm}^{-1}$ as well as weaker peaks at $1161~{\rm and}~922~{\rm cm}^{-1}$ (Fig. 4). Formation of this product was seen after irradiation with electrons with energies as low as 7 eV (electron dose of $2.4~{\rm x}~10^3~\mu{\rm C}$), suggesting that electron impact ionization cannot be the sole mechanism for dimethyl ether formation. During annealing experiments, IR peaks at $1161~{\rm and}~922~{\rm cm}^{-1}$, associated exclusively with CH₃OCH₃, began to disappear at $\sim 100~{\rm K}$, consistent with results of post-irradiation TPD.

In previous IRAS studies of irradiated CH₃OH, the peaks at 1161 and 922 cm⁻¹ were attributed to either dimethyl ether (Oberg et al. 2009) or another methanol radiolysis product, methyl formate (HCOOCH₃) (Gerakines et al. 1995; Palumbo et al. 1999; Bennett et al. 2007). In order to resolve this discrepancy, IR spectra of condensed film of a mixture of \sim 20 per cent (v/v) dimethyl ether in CH₃OH were compared to those of a mixture of \sim 30 per cent (v/v) methyl formate in CH₃OH. IR peaks of the dimethyl ether/CH₃OH thin fil better matched those of the electron irradiated CH₃OH ice (Fig. 5). Although IR features of the methyl formate also align well with features in the irradiated CH₃OH sample, particularly the band at 1161 cm⁻¹, the absence of the even more prominent methyl formate peak at 1207 cm⁻¹ in the irradiated CH₃OH sample supports our IR peak assignments (Chen et al. 2013).

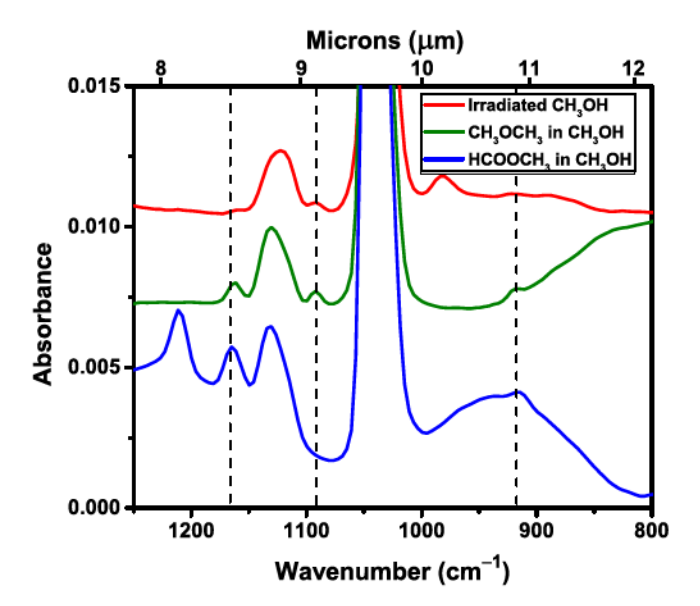


Figure 5. IRAS scan of (1) 100 ML of CH₃OH after irradiation with 14 eV electrons for 20 min at a transmitted current of 2 μ A (red curve), (2) CH₃OH / CH₃OCH₃ (dimethyl ether) mixture (green curve), (3), CH₃OH / HCOOCH₃ (methyl formate) mixture (blue curve).

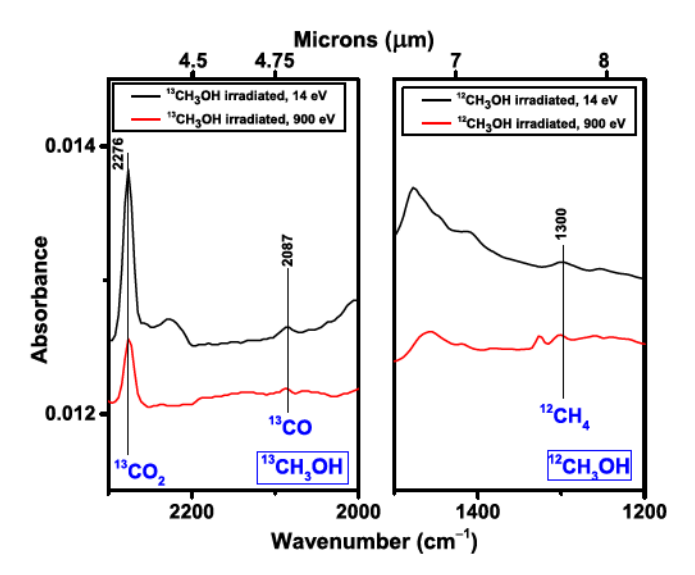


Figure 6. IRAS scan of 100 ML of 13 CH₃OH (left-hand panel) and 12 CH₃OH (right-hand panel) irradiated with 14 eV electrons for 120 min at a transmitted current of 2 μ A (black curve) and with 900 eV electrons for 2 min at a transmitted current of 0.5 μ A (red curve).

Dimethyl ether formation likely occurs via radical-radical reactions involving CH₃O• and •CH₃ radicals (Bennett et al. 2007).

3.4 Hydroxymethyl radical (•CH2OH) formation

Consistent with the results of multiple previous IRAS studies of irradiated methanol ices (Gerakines et al. 1996; Bennett et al. 2007; Oberg et al. 2009; de Barros et al. 2011), the hydroxymethyl radical (•CH₂OH) was identifie at 85 K by a single weak peak at 1196 cm⁻¹ following high-energy and low-energy electron irradiation of condensed methanol. Tentative evidence for the production of hydroxymethyl radical was only seen after irradiation with 14 eV electrons (electron dose of 2.4 \times 10³ μ C) (Fig. 4), although formation of HOCH₂CH₂OH was detected at energies as low as 7 eV. The observed difference in threshold incident electron energy may be due to a higher minimum IR detectability of hydroxymethyl radical compared to that of ethylene glycol. Hydroxymethyl radical has been identifie in several methanol radiolysis studies involving electron spin resonance spectroscopy studies following spin trapping (Spinks & Woods 1990).

3.5 CO₂ formation

Using IRAS, carbon dioxide (CO₂) was detected following both high-energy and low-energy electron irradiation of methanol ices. IR evidence for CO₂ production when condensed methanol was irradiated with low-energy (14 eV) electrons was detected only following a high total electron dose of $1.4 \times 10^4 \ \mu \text{C}$. Background signals for CO₂ present in our experimental setup necessitated the use of $^{13}\text{CH}_3\text{OH}$ in order to detect IR peaks uniquely attributable to carbon dioxide produced from the radiolysis of methanol. A prominent IR peak at 2276 cm⁻¹ was assigned to $^{13}\text{CO}_2$ (Fig. 6), in good agreement with literature values (Table 1) (Gerakines et al. 1996). Carbon dioxide is thought to be produced by the reaction of

CO and the hydroxyl radical (•OH) formed during the radiolysis of methanol (Garrod & Herbst 2006).

3.6 CO formation

Irradiation of methanol ices by both high- and low-energy electrons resulted in the formation of carbon monoxide (CO), as shown by IRAS results. Similar to CO₂, an IR peak attributable to carbon monoxide was detected at 85 K only after irradiation of condensed methanol with a high total electron dose $(1.4 \times 10^4 \ \mu\text{C})$ of low-energy (14 eV) electrons. A much smaller dose of 60 μ C with higher energy (900 eV) electrons incident on condensed methanol was sufficien to generate CO. A single IR peak in both irradiated CH₃OH (at 2134 cm⁻¹) (data not shown) and ¹³CH₃OH (at 2087 cm⁻¹) (Fig. 6) thin f lms was attributed to carbon monoxide, in good agreement with previously published values (Table 1; Allamandola et al. 1988; Gerakines et al. 1996; Palumbo et al. 1999; Hudson and Moore 2000; Baratta et al. 2002; Oberg et al. 2009; de Barros et al. 2011). Dissociation of the formyl radical (•HCO) is thought to yield CO (Oberg et al. 2009).

3.7 CH₄ formation

Using IRAS, methane (CH₄) was detected following both high-energy and low-energy electron irradiation of methanol ices. A high total electron dose ($1.4 \times 10^4 \ \mu C$) was also necessary to detect formation of methane in CH₃OH thin film irradiated with low-energy (14 eV) electrons at 85 K. We attribute the detection of methane at such a high temperature to methane trapping within methanol ices. A single IR peak at 1303 cm⁻¹ was attributed to CH₄ (Fig. 6), in good agreement with previously published values (Table 1) (Table 1; Allamandola et al. 1988; Gerakines et al. 1996; Palumbo et al. 1999; Hudson and Moore 2000; Baratta et al. 2002; Oberg et al. 2009; de Barros et al. 2011). Methane formation is ascribed to the combination of •CH₃ and •H radicals (Oberg et al. 2009).

3.8 Reconciling post-irradiation IR and TPD data

As described in detail in our previous publication (Boamah et al. 2014), results of TPD experiments conducted following 20 eV electron irradiation of condensed methanol indicate the formation of several additional products: acetaldehyde (CH₃CHO), methyl formate (HCOOCH₃), glycolaldehyde (HOCH₂CHO), acetic acid (CH₃COOH), methoxymethanol (CH₃OCH₂OH), ethanol (CH₃CH₂OH), glycolic acid (HOCH₂CO₂H), and 1,2,3-propanetriol (HOCH₂CHOHCH₂OH, glycerol). Following 1000 eV electron irradiation of methanol ices, we have identifie using TPD experiments (Fig. 2) all the above-mentioned products, except acetaldehyde. We attribute this discrepancy to the challenges associated with using TPD, and conclude that post-irradiation TPD results indicate the same products are formed following low-energy (20 eV) and high-energy (1000 eV) electron irradiation of condensed methanol.

While seven methanol radiolysis products were identifie with IR, as described in detail in Sections 3.1 to 3.7, clear IR signatures were not found for the eight products mentioned in the current section. This discrepancy between post-irradiation IR and TPD data is not surprising given that (1) an observed infrared feature is generally associated with normal modes of two or more atoms rather than a specifi molecule, (2) IRAS signals are typically small even for surface coverages in the multilayer regime, (3) irradiated methanol

¹ More conclusive IR evidence for the production of hydroxymethyl radicals was seen following irradiation of methanol ices with higher energy (>17 eV) electrons.

Downloaded from http://mnras.oxfordjournals.org/ at Harvard Library on June 29, 2016

Table 1. Comparison of several studies which investigated the radiolysis/photolysis of CH₃OH thin film using IRAS. Expansion of a previously published table (Bennett et al. 2007).

	•		J)	•		•			
			Jheeta et al.	Bennett	Allamandola	Oberg et al.	Gerakines	Chen et al.	Hudson and	Palumbo	Baratta et al.	de Barros
		This work	(2013)	et al. (2007)	et al. (1988)	(2009)	et al. (1996)	(2013)	Moore (2000)	et al. (1999)	(2002)	et al. (2011)
		Electrons	Electrons	Electrons				X-rays	Protons	He ⁺ ions	He ⁺ ions	Ions
		14 eV	$1 \mathrm{keV}$	5 keV	ΔŊ	ΔΩ	ΔΩ	$\sim\!400\mathrm{eV}$	$0.8\mathrm{MeV}$	$3 \mathrm{keV}$	3 keV	16-774 MeV
	Temperature	85 K	30 K	11 K			10-230 K	14-210 K	16 K	10-200 K	10-20 K	15 K
v4	СН20Н	1195	1345(?)	1192		1195	1197	1193				1193
44	H_2CO	1724	1724	1726	1720	1727	1719	1726	1712	1720	1720	1726
v 3	H_2CO			1496	1500	1498	1497	1498	1499			1497
v 2	H_2CO	1250		1245		1245	1244	1249	1248			1244
1 1	НСО			1849, 1841	1850	1843	1850, 1863	1842	1848			
1 1	00	2134	2136	2134	2137	2135	2138	2134	2135	2136	2136	2136
1 1	$CO(^{13}C)$	2087					2092					2092
v 3	CO ₂	2341	2341	2345	2343	2340	2342	2340	2341	2344	2344	2342
v 3	CO_2 (13 C)	2276					2278					
n 2	co_2				657		655		654	099		
74	CH_4	1303	1304	1303	1304	1301	1304	1304	1303	1305	1308	
v 3	CH ₄				3012		3011					3009
114	CH_3OCHO			1718			1718	1726				
V12	СН3ОСНО					1214						
75	CH_3OCHO			916		911	910					
108	CH_3OCHO			1160			1160	1161				1160
V10	CH_3OCH_3	1161				1161		1161				
94	CH_3OCH_3	914				921						
64	$HOCH_2CH_2OH$	1092		1090		1090	1088	1090	1088			
74	$HOCH_2CH_2OH$	891		688		890		875–932	885			
94	$HOCH_2CH_2OH$	864		928		998			861			
75	$HOCH_2CH_2OH$			525					524			
V14	$HCOCH_2OH$			1747				1746				
V12	CH_3CH_2OH					1382						
44	CH_3CH_2OH					885						
v 2	C_2H_6					1372						
V12	C_2H_6					822						
17	СН3СНО					1350						
V18	CH_3COCH_3									1720		
117	CH ₃ COCH ₃									1444		
V11	CH_3COCH_3									1232		
v 10	CH_3COCH_3									1090		
v ₁	H_2 ?						4140					
v 2	HC00-3					1382			1384			
75	HC00-?								1589			
n 2	H_2O									1655	1655	
Note.	Note. '?' refers to ambiguous assignments.	assignments.										

contains 15 or more radiolysis products which engender a multitude of often overlapping IR peaks, and (4) methoxymethanol is a labile species for which there is no IR spectrum in databases.

Despite the absence of IRAS evidence for acetaldehyde (CH₃CHO), methyl formate (HCOOCH₃), glycolaldehyde (HOCH2CHO), methoxymethanol (CH3OCH2OH), and ethanol (CH₃CH₂OH) at 85 K, we suggest that thermal processing above 85 K of the irradiated methanol fil is not necessary for the formation of these fi e products. Our reasoning is based on the assumption that barrierless radical-radical reactions are thought to yield the photolysis/radiolysis products of methanol. Therefore, the diffusion barriers of the radicals determine the temperature dependence of product formation. Our results indicate that these fi e radiolysis products must form at 85 K or below given that the methoxy (CH₃O•), formyl (•HCO), and methyl (•CH₃) radicals have diffusion barriers (Garrod et al. 2008) significantl lower than that of the hydroxymethyl radical (•CH2OH), whose dimerization yields ethylene glycol at 85 K or below, as verifie by IR data presented herein.

3.9 Implications for interstellar chemistry

The results presented herein suggest that low-energy secondary electrons can induce chemical processes within interstellar ice films. Within protostellar environments, cosmic-ray induced low-energy secondary electrons may interact with ice f lms rich in CH₃OH to form radical species whose subsequent reactions may lead to the production of some of the diverse observed interstellar molecules, including prebiotic species. Because all previous studies (Allamandola et al. 1988; Gerakines et al. 1996; Oberg et al. 2009) have failed² to identify methoxymethanol (CH₃OCH₂OH) as a photolysis product of condensed methanol, this electron-induced product of condensed methanol (Harris et al. 1995; Boamah et al. 2014; Boyer et al. 2014; Maity, Kaiser & Jones 2015) could serve as a tracer molecule for electron-induced reactions in the ISM.

Although current astrochemical simulations model the irradiation chemistry of ice-covered interstellar dust grains by ionizing radiations such as cosmic-rays (e.g., Abdulgalil et al. 2013), no simulations have taken into account the role of low-energy secondary electrons. The kinetic (stochastic) from the outset Monte Carlo method (e.g., Chang, Cuppen & Herbst 2005) must be modifie to model the attenuation of low-energy electrons in ice, predicting both the spatial location and the nature of the energy transfer events.

4 CONCLUSIONS

We have investigated the effects of high-energy and low-energy electron irradiation of nanoscale thin f lms of CH₃OH at 85 K under UHV conditions. Infrared spectroscopy results indicate that ethylene glycol, formaldehyde, dimethyl ether, carbon dioxide, carbon monoxide, methane, and the hydroxymethyl radical are nascent low-and high-energy electron-induced radiolysis products of condensed methanol at 85 K. Post-irradiation TPD results presented herein also demonstrate that the same radiolysis products result from irradiation of condensed methanol with low-energy (<20 eV) and high-energy (1000 eV) electrons, suggesting that high-energy radiation-induced

changes are attributable to low-energy secondary electron interactions with condensed matter. We speculate that qualitatively similar results will result for analogues of cosmic methanol ices containing both CO and water. Therefore, the results presented herein may have implications for the synthesis of COM in extra-terrestrial ices.

ACKNOWLEDGEMENTS

This work was supported by grants from the National Science Foundation (NSF grant number CHE-1012674 and CHE-1005032) and Wellesley College (Faculty awards and Brachman Hoffman small grants). KKS gratefully acknowledges funding from 'Sally Etherton Cummins' 58 Summer Science Research Fellowship Fund'. We thank an anonymous referee for numerous constructive comments on the paper. CRA dedicates this contribution to his late great grandfather, Professor Allen Abraham, who was in 1911 one of the first astronomers from Asia to be elected as a Fellow of the Royal Astronomical Society (FRAS) for his seminal contributions to calculating the trajectory of Haley's comet in 1910.

REFERENCES

Abdulgalil A. G. M. et al., 2013, Philos. Trans. A, 371, 20110586

Allamandola L. J., Hudgins D. M., 2000, Solid State Astrochemistry, From Interstellar Polycyclic Aromatic Hydrocarbons and Ice to Astrobiology. Springer, Netherlands

Allamandola L. J., Sandford S. A., Valero G. J., 1988, Icarus, 76, 225

Andrade D. P. P., Boechat-Roberty H. M., Martinez R., Homem M. G. P., da Silveira E. F., Rocco M. L. M., 2009, Surf. Sci., 603, 1190

Arumainayagam C. R., Lee H. D., Nelson R. B., Haines D. R., Gunawardane R., 2010, Surf. Sci. Rep., 65, 1

Baratta G. A., Leto G., Palumbo M. E., 2002, A&A, 384, 343

Bennett C. J., Chen S.-H., Sun B.-J., Chang A. H. H., Kaiser R. I., 2007, ApJ, 660, 1588

Bisschop S. E., Fuchs G. W., van Dishoeck E. F., Linnartz H., 2007, A&A, 474, 1061

Boamah M. D. et al., 2014, Faraday Discuss., 168, 249

Bockeleemorvan D., Colom P., Crovisier J., Despois D., Paubert G., 1991, Nature 350, 318

Boyer M. C., Boamah M. D., Sullivan K. K., Arumainayagam C. R., Bazin M., Bass A. D., Sanche L., 2014, J. Phys. Chem. C, 118, 22592

Charnley S. B., Tielens A. G. G. M., Millar T. J., 1992, ApJ, 399, L71

Chang Q., Cuppen H. M., Herbst E., 2005, A&A, 434, 599

Chen Y. J., Ciaravella A., Caro G. M. M., Cecchi-Pestellini C., Jiménez-Escobar A., Juang K. J., Yih T. S., 2013, ApJ, 778, 162

Cuppen H. M., 2014, Faraday Discuss., 168, 571

de Barros A. L. F., Domaracka A., Andrade D. P. P., Boduch P., Rothard H., da Silveira E. F., 2011, MNRAS, 418, 1363

de Barros A. L. F., da Silveira E. F., Pilling S., Domaracka A., Rothard H., Boduch P., 2014, MNRAS, 438, 2026

Dempster A. B., Zerbi G., 1971, J. Chem. Phys., 54, 3600

Ehrenfreund P., Charnley S. B., 2000, ARA&A, 38, 427

Friberg P., Hjalmarson A., Madden S. C., Irvine W. M., 1988, A&A, 195, 281

García-Hernández D. A., Cataldo F., Manchado A., 2013, MNRAS, 434, 415

Garrod R. T., Herbst E., 2006, A&A, 457, 927

Garrod R. T., Widicus S. L., Herbst E., 2008, ApJ, 682, 283

Gerakines P. A., Schutte W. A., Ehrenfreund P., 1996, A&A, 312, 289

Gerakines P. A., Schutte W. A., Greenberg J. M., van Dishoeck E. F., 1995, A&A, 296, 810.

Getoff N., Ritter A., Schworer F., Bayer P., 1993, Radiat. Phys. Chem., 41,

Gibb E. L., Whittet D. C. B., Boogert A. C. A., Tielens A. G. G. M., 2004, ApJS, 151, 35

² It is possible that these authors did not specificall look for methoxymethanol in their UV photolysis studies. A clear non-detection of this species from the UV photolysis of condensed methanol is necessary to unambiguously identify CH₃OCH₂OH as a radiolysis tracer.

672

- Grim R. J. A., Baas F., Geballe T. R., Greenberg J. M., Schutte W., 1991, A&A, 243, 473
- Harris T. D., Lee D. H., Blumberg M. Q., Arumainayagam C. R., 1995, J. Phys. Chem., 99, 9530
- Herbst E., 1995, Annu. Rev. Phys. Chem., 46, 27
- Herbst E., 2014, Phys. Chem. Chem. Phys., 16, 3344
- Hollis J. M., Lovas F. J., Jewell P. R., 2000, ApJ, 540, L107
- Horn A., Mollendal H., Sekiguchi O., Uggerud E., Roberts H., Herbst E., Viggiano A. A., Fridgen T. D., 2004, ApJ, 611, 605
- Hudson R. L., Moore M. H., 2000, Icarus, 145, 661
- Irvine W. M., Goldsmith P. F., Hjalmarson A. A., 1987, in Dordrecht D., ed., Interstellar Processes, Chemical Abundances in Molecular Clouds. Reidel, Dordrecht
- Jheeta S., Domaracka A., Ptasinska S., Sivaraman B., Mason N. J., 2013, Chem. Phys. Lett., 556, 359
- Kaplan I. G., Miterev A. M., 1987, Adv. Chem. Phys., 68, 255
- Kurtz R. L., Usuki N., Stockbauer R., Madey T. E., 1986, J. Electron Spectrosc., 40, 35
- Maity S., Kaiser R. I., Jones B. M., 2015, Phys. Chem. Chem. Phys., 17, 3081
- Mangum J. G., Wootten A., 1993, ApJS, 89, 123

- Mannings V., Boss A. P., Russell S. S., 2000, Protostars and Planets IV. Univ. Arizona Press, Tucson, AZ
- Maret S., Ceccarelli C., Tielens A. G. G. M., Caux E., Lefloc B., Faure A., Castets A., Flower D. R., 2005, A&A, 442, 527
- Oberg K. I., Garrod R. T., van Dishoeck E. F., Linnartz H., 2009, A&A, 504, 819
- Oberg K. I., Boogert A. C. A., Klaus M. P., Saskia van den B., Ewine F.v.D., Sandrine B., Geoffrey A. B., Neal J. E. II, 2011, ApJ, 740, 109
- Olano C. A., Wlamsley C. M., Wilson T. L., 1988, A&A, 196, 194
- Palumbo M. E., Castorina A. C., Strazzulla G., 1999, A&A, 342, 551
- Pimblott S. M., LaVerne J. A., 2007, Radiat. Phys. Chem., 76, 1244
- Prasad S. S., Tarafdar S. P., 1983, ApJ, 267, 603
- Spinks J. W. T., Woods R. J., 1990, An Introduction to Radiation Chemistry. Wiley, New York
- van Dishoeck E. F., Jansen D. J., Phillips T. G., 1993, A&A, 279, 541 Vidali G., 2013, Chem. Rev., 113, 8762
- Watanabe N., Shiraki T., Kouchi A., 2003, ApJ, 588, 121

This paper has been typeset from a TEX/LATEX f le prepared by the author.